Biochemical Pharmacology, Vol. 46, No. 3, pp. 503–510, 1993.
Printed in Great Britain.

0006-2952/93 $6.00 + 0.00

TRANSPORT OF 5-FLUOROURACIL AND URACIL INTO HUMAN ERYTHROCYTES

BARBARA A. DOMIN,* WILLIAM B. MAHONY and THOMAS P. ZIMMERMAN
Division of Experimental Therapy, Wellcome Research Laboratories, Research Triangle Park, NC 27709, U.S.A.

(*Received* 8 *January* 1993; *accepted* 26 *March* 1993)

Abstract—The transport of 5-fluorouracil (5-FU) and uracil into human erythrocytes has been investigated under initial velocity conditions with an "inhibitor-stop" assay using a cold papaverine solution to terminate influx. At 37° and pH 7.3, 5-FU influx was nonconcentrative; was partially inhibited by adenine, hypoxanthine, thymine, and uracil; and was insensitive to inhibition by nucleosides or inhibitors of nucleoside transport. Inhibition of the influx of 5-FU or uracil by adenine (3.0 mM) did not increase when other pyrimidines or inhibitors of nucleoside transport were combined with adenine. 5-FU and uracil exhibited similar saturable ($K_m \sim 4$ mM, $V_{max} \sim 500$ pmol/sec/5 μL cells) and nonsaturable (rate constant ~ 80 pmol/sec/mM/5 μL cells) components of influx. 5-FU, uracil, adenine, and hypoxanthine were competitive inhibitors of each other's influx with K_i values matching their respective K_m values for influx. We conclude that 5-FU and uracil enter human erythrocytes at similar rates via both nonfacilitated diffusion and the same carrier that transports adenine and hypoxanthine.

5-Fluorouracil (5-FU†) is one of the most effective agents in the treatment of various solid tumors such as colorectal cancer [1]. The biochemical pharmacology of 5-FU has been reviewed recently [2, 3]. The uptake of 5-FU or the related physiological pyrimidine uracil (Ura) has been examined in a variety of cell and tissue types with differing results. Uptake of Ura in cultured cells reportedly occurs via a nonconcentrative, saturable mechanism [4–7], or via nonfacilitated diffusion [8, 9]. 5-FU uptake has been reported to occur via the same nonconcentrative, saturable carrier as Ura [7], via an active, concentrative mechanism [10], or via nonfacilitated diffusion [8, 9]. *In vivo* tissue or tumor uptake of 5-FU is pH dependent and reportedly occurs via nonfacilitated diffusion at physiological pH [11]. Trapping of nonmetabolized 5-FU in tumors has also been observed [12–14]. Uptake of Ura or 5-FU by intestinal preparations was by both a saturable and a nonsaturable process [15–23], with the saturable process being active and concentrative [15, 17–23] and sodium dependent [18–20]. In a previous study with human erythrocytes, the number of independent carriers involved in the transport of purine and pyrimidine nucleobases could not be determined [24]. We have used a novel "inhibitor-stop" assay [25], which permits initial velocity measurements, to demonstrate previously that adenine (Ade), hypoxanthine (Hyp), and guanine (Gua) enter human erythrocytes by a single carrier and by nonfacilitated diffusion. Also, pyrimidine nucleobases partially inhibit purine nucleobase transport in these cells [25]. To define better the permeation characteristics of 5-FU, we investigated the influx of 5-FU and Ura in human erythrocytes using this "inhibitor-stop" assay. In this study, we present evidence that 5-FU and Ura enter human erythrocytes by the same carrier that transports purine nucleobases and by nonfacilitated diffusion.

* Corresponding author. Tel. (919) 248-8028; FAX (919) 248-8747.

† Abbreviations: Ade, adenine; 5-FU, 5-fluorouracil; Gua, guanine; Hepes, 4-(2-hydroxyethyl)-1-piperazineethanesulfonic acid; Hyp, hypoxanthine; NBMPR, 6-[(4-nitrobenzyl)thio]-9-β-D-ribofuranosylpurine; and Ura, uracil.

MATERIALS AND METHODS

Materials. [6-^{3}H]5-FU (15 Ci/mmol), [G-^{3}H]Hyp (26 Ci/mmol), [U-^{14}C]sucrose (4 Ci/mol), and [^{3}H]-water (1 mCi/g) were from Dupont–New England Nuclear (Boston, MA). [5,6-^{3}H]Ura (47 Ci/mmol) was from ICN Biomedicals (Costa Mesa, CA) and [8-^{3}H]Ade (24 Ci/mmol) was from Amersham Corp. (Arlington Heights, IL). Dilazep was provided by Hoffmann–LaRoche (Nutley, NJ). 4-(2-Hydroxyethyl)-1-piperazineethanesulfonic acid (Hepes) was from GIBCO (Grand Island, NY). Sep-Pak® C_{18} cartridges were from Waters Associates (Milford, MA). Unlabeled nucleobases and nucleosides, papaverine hydrochloride, dipyridamole, and 6-[(4-nitrobenzyl)thio]-9-β-D-ribofuranosylpurine (NBMPR) were from Sigma (St. Louis, MO). All other chemicals were reagent grade quality. All solutions were prepared in 10 mM Hepes:0.9% NaCl buffer, pH 7.3. [^{3}H]Ade and [^{3}H]Hyp were purified on Sep-Pak C_{18} cartridges as described previously [25] to >96% purity as determined by reversed-phase HPLC. [^{3}H]5-FU and [^{3}H]Ura were >99% pure.

Preparation of human erythrocytes. Human erythrocytes were obtained from healthy volunteers, prepared as described previously [25, 26] and

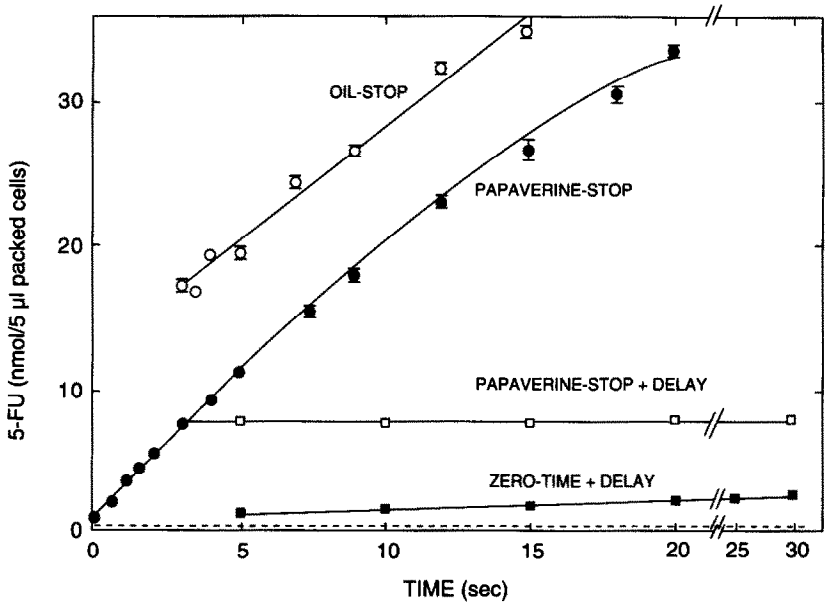

Fig. 1. Efficacy of a cold papaverine solution as a "stopper" for 5-FU influx. Human erythrocytes (5 µL packed cells) were incubated at 37° in 10 mM Hepes in 0.9% NaCl buffer, pH 7.3, with 20 mM [^{3}H]5-FU (0.27 Ci/mol) in a total volume of 100 µL. Each time point is the mean ± SEM of triplicate values and error bars were omitted when they did not extend beyond the symbol boundaries. The "oil-stop" method [25, 27, 28] used the initiation of centrifugation as the assay termination time, with no attempt to correct for the time required for sedimentation of the cells into the oil phase. The "papaverine-stop" method [25] used the addition of 700 µL of the cold saturated papaverine solution as the assay termination time, and centrifugation of the cells through oil was initiated 10 sec after the papaverine addition. For both of these conditions, the time indicated in the graph is the assay termination time. The two conditions used for determining the efficacy of the assay termination were as follows: (1) Papaverine-stop + delay (□): Cells were incubated for 3.0 sec with the [^{3}H]5-FU. The papaverine solution was then added, and cells were kept at room temperature for 10 sec plus the additional times indicated in the graph before centrifugation. (2) Zero-time + delay (■): The papaverine solution was added to the cells before the [^{3}H]5-FU, and the cells were kept at room temperature for the times indicated in the graph before centrifugation. [^{14}C]Sucrose space is represented by the dashed line.

resuspended in 10 mM Hepes in 0.9% NaCl, pH 7.3, to a final hematocrit of 25%.

Kinetics of permeant influx. Influx assays were performed at 37° with the "inhibitor-stop" method as described previously [25]. Initial velocities of influx were calculated by linear regression analysis of the slopes of plots of cell-associated radioisotope versus four assay times within the linear phase of permeant influx: 0, 1.0, 2.5, and 5.0 sec for 5-FU; 0, 1.0, 2.0, and 4.0 sec for Ura; 0, 0.5, 1.0, and 1.5 sec for Ade; and 0, 0.5, 1.0, and 1.0 sec for Hyp.

"Oil-stop" assays [27] of 5-FU influx were performed, where indicated, with the modifications described previously [25, 28].

The amount of extracellular radioactivity in the cell pellet was determined using [^{14}C]sucrose [26] with the "inhibitor-stop" method. Intracellular [^{3}H]-water space was determined with the "oil-stop" assay [27].

Kinetic analysis. Kinetic parameters were determined by nonlinear regression [29, 30] with one or more of the following equations using a $1/v^2$ weighting factor:

$$v = \frac{(V_{max})(S)}{S + K_m} + (c)(S). \quad (1)$$

Competitive inhibition:

$$v = \frac{(V_{max})(S)}{S + K_m(1 + I/K_i)} + (c)(S). \quad (2)$$

Noncompetitive inhibition:

$$v = \frac{(V_{max})(S)}{S(1 + I/K_i) + K_m(1 + I/K_i)} + (c)(S). \quad (3)$$

"c" is the rate constant for a nonsaturable component of permeant influx. The concentration dependence of influx rates in the absence of inhibitors was analyzed with Equation 1. When inhibitors were present, analysis was performed with both Equations 2 and 3, and P values for competitive versus noncompetitive inhibition were obtained as described

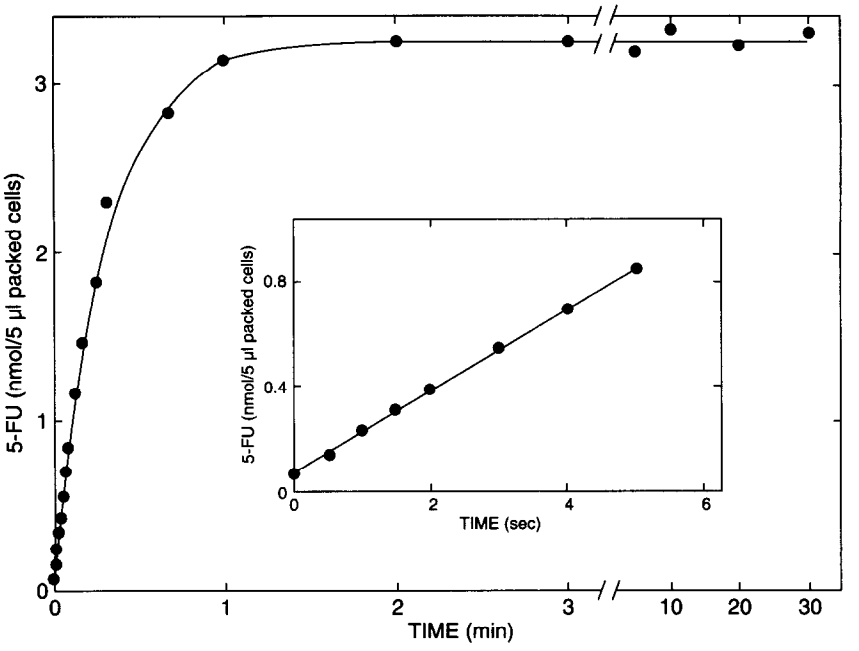

Fig. 2. Time dependence of 5-FU influx. Human erythrocytes were incubated at 37° for the indicated times with 1.0 mM [^{3}H]5-FU (5.1 Ci/mmol) as described in Materials and Methods. Each time point is the mean of duplicate assays and the deviation from the mean did not exceed 12%.

previously [29, 30]. A small P value indicates that the more complex model (noncompetitive inhibition) fits the data better than the simpler model [30].

Analysis of inhibition of permeant influx. Statistical comparisons of influx rates were determined with the PROC GLM computer program from the SAS Institute, Inc. (Cary, NC).

Metabolism studies. Cells were incubated for 15 min with [^{3}H]5-FU (7.6 µM, 2 Ci/mmol; or 30 mM, 0.4 Ci/mol) and [^{3}H]Ura (8.9 µM, 19 Ci/mmol) under the same conditions used for influx experiments. Each incubation was terminated with 700 µL of the ice-cold saturated papaverine solution, and the cell-associated radioactivity was extracted with cold trichloroacetic acid [25]. Extracts were analyzed by chromatography with reversed-phase HPLC [31].

RESULTS

Efficacy of the "inhibitor-stop" assay for measuring 5-FU and Ura influx. The influx of 20 mM [^{3}H]5-FU was measured with both an "oil-stop" assay and the "inhibitor-stop" assay (Fig. 1). At this concentration, influx of 5-FU was linear with time for at least 5 sec. The influx rates obtained with these two methods appeared similar, thus supporting the assumption that the addition of papaverine did not interfere with the measurement of cell-associated [^{3}H]5-FU. A small leakage of 5-FU across the membrane occurred after adding the cold papaverine solution to the cells (Fig. 1, open and closed squares). This accounted for a zero-time value for 5-FU that was 1.9-fold higher than the sucrose space (Fig. 1, dashed line). However, this leakage rate was <2% of the total influx rate of 5-FU and, as discussed previously [25, 29], was insignificant for 5-FU influx rate determinations as long as the time interval between addition of papaverine and centrifugation of the cells was <15 sec. Similar results were observed with 20 mM Ura (data not shown).

Metabolism. Metabolism of [^{3}H]5-FU (7.6 µM or 30 mM) was examined after 15-min incubations with human erythrocytes at 37°. In each case, >98% of the cell-associated radioactivity was eluted from the reversed-phase HPLC column at the same retention time as that of the authentic standard of 5-FU. Since it is recognized that natural pyrimidines are not metabolized in human erythrocytes [24], the metabolism of Ura was examined only at a low concentration. After 15-min incubations of 8.9 µM [^{3}H]Ura with human erythrocytes, >98% of the permeant found intracellularly was intact Ura.

Time dependence of 5-FU influx. [^{3}H]5-FU (1.0 mM) equilibrated across the erythrocyte membrane within 2 min (Fig. 2), and the intracellular concentration at equilibrium (900 pmol/µL cell water) was approximately equal to the extracellular concentration.

Effects of nucleobases, nucleosides, and inhibitors of nucleoside transport on the influx of 5-FU. Nucleobases significantly inhibited (up to 60% inhibition) the influx of 1.2 µM [^{3}H]5-FU, and the degree of inhibition decreased with increasing permeant concentrations (Table 1). By contrast, nucleosides or inhibitors of nucleoside transport inhibited 5-FU influx by ≤20%. Combinations of

Table 1. Effects of nucleobases, nucleosides, and inhibitors of nucleoside transport on the influx of 5-FU in human erythrocytes

Additive	[^{3}H]5-FU 1.2 μM*	1.0 mM†	20 mM‡
	% Inhibition		
Adenine (1.0 mM)	56§	45§	30§
Adenine (3.0 mM)	57§	48§	26§
Hypoxanthine (1.0 mM)	52§	38§	22§
Thymine (3.0 mM)	47§	28§	21§
Thymine (6.0 mM)	42§	35§	26§
Orotic acid (0.9 mM)	8‖	5	14‖
Uracil (6.0 mM)	31§		1
5-FU (20 mM)	44§¶		11‖¶
Cytosine (6.0 mM)	11‖		15‖
Thymidine (1.0 mM)	18§	15§	7
Uridine (1.0 mM)	15§	11**	20**
5-Fluorouridine (1.0 mM)	0		3
5-Fluorodeoxyuridine (1.0 mM)	2		2
NBMPR (1.0 μM)††	8‖		9
Dipyridamole (1.0 μM)††	13§	6	19‖
Dilazep (1.0 μM)††	6	11‖	15‖

The initial velocity of influx of [^{3}H]5-FU was determined at 37° as described under Materials and Methods. Compounds were added simultaneously with the radiolabeled permeant, except where indicated. No correction was made for the contribution of nonfacilitated diffusion which was calculated to be 41, 52 and 74% of the total influx for 1.2 μM, 10 mM, and 20 mM 5-FU, respectively.

* Control rate was 0.24 ± 0.04 pmol/sec/5 μL packed cells.

† Control rate was 150 ± 10 pmol/sec/5 μL packed cells.

‡ Control rate was 2200 ± 300 pmol/sec/5 μL packed cells.

§ Significantly different from control value, $P < 0.0001$.

‖ Significantly different from control value, $P < 0.001$.

¶ These values were obtained without correcting for changes in specific activities.

** Significantly different from control value, $P < 0.05$.

†† Cells were preincubated with inhibitor 20 min prior to addition of radiolabeled permeant.

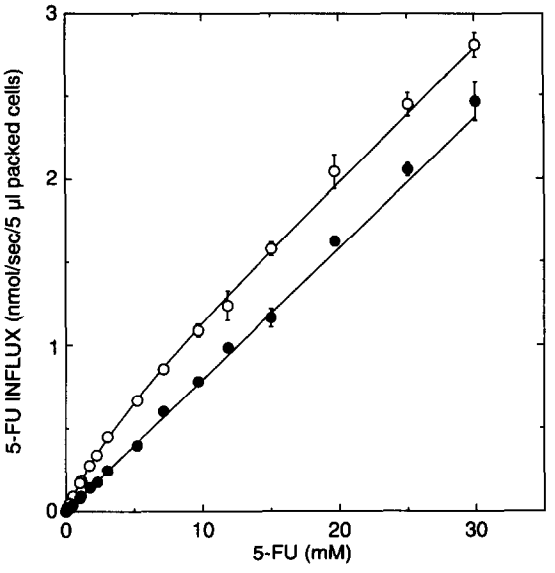

Fig. 3. Concentration dependence of 5-FU influx. Assays were performed at 37° in the absence (○) or presence (●) of 3.0 mM Ade. [^{3}H]5-FU concentrations were 5.0 μM to 30 mM (0.55 or 36 Ci/mol). Velocities were determined by linear regression analysis of data obtained during the linear phase of influx as described in Materials and Methods. Error bars represent the standard errors of the slopes obtained with this analysis, and these were omitted where they did not extend beyond the symbol boundaries. The fitted lines are those derived by nonlinear regression analysis using Equation 2 and a K_i value for Ade of 12 μM (Table 2).

3.0 mM Ade *and* 1.0 μM dilazep, 2.3 mM Hyp, 20 mM unlabeled 5-FU, 6.0 mM thymine, or 1.0 mM Ura failed to inhibit further the influx of 1.2 μM, 1.0 mM, or 20 mM 5-FU beyond the inhibition observed with 3.0 mM Ade alone (data not shown).

Concentration dependence of 5-FU influx. The rate of 5-FU influx was examined at concentrations from 5.0 μM to 30 mM in the absence and presence of 3.0 mM Ade (Fig. 3). In the absence of Ade, the rate of 5-FU influx increased with 5-FU concentration in a biphasic manner: hyperbolic at concentrations <10 mM and linear at concentrations >10 mM. In the presence of Ade, the rate of 5-FU influx increased linearly with 5-FU concentration and was inhibited from 12 to 60% over the range of permeant concentrations shown. These observations are consistent with the presence of both a saturable and nonsaturable influx mechanism. These data were analyzed by nonlinear regression using two approaches: (a) data obtained in the absence of Ade analyzed with Equation 1, and (b) all data (i.e. in the absence and presence of Ade) analyzed with Equation 2 for competitive inhibition where the K_i for adenine was defined as a constant with a value of 12 μM [25]. Similar values for each influx kinetic parameter were obtained using both of these analyses (Table 2).

Characterization of Ura influx. The influx of 1.0 mM [^{3}H]Ura was also nonconcentrative, with an intracellular concentration of 940 pmol/μL cell water at equilibration. As seen with 5-FU, Ura influx was inhibited by Ade (≤50%) but not by dilazep. Inhibition by Ade (3.0 mM) was not further enhanced by the addition of 5-FU, unlabeled Ura, or dilazep (data not shown). The pattern of concentration dependence (Fig. 4) of Ura influx was similar to that of 5-FU, i.e. saturable (K_m = 4.0 ± 0.4 mM, V_{max} = 400 ± 40 pmol/sec/5 μL cells) and nonsaturable (c = 70 ± 1 pmol/sec/mM/5 μL cells).

Kinetic evidence that 5-FU and Ura are permeants of the same carrier that transports Ade and Hyp. At permeant concentrations above influx K_m values, nonfacilitated diffusion of 5-FU and Ura was ≥50% of the total influx. Nevertheless, inhibition of the influx of both of these permeants by Ade or Hyp could be analyzed by nonlinear regression. In all

Table 2. Analyses of kinetic parameters for 5-FU influx

Equation	Variables	Fixed constant	K_m (mM)	V_{max} (pmol/sec/5 μL cells)	c (pmol/sec/mM 5-FU/5 μL cells)
1*	K_m, V_{max}, c		4.2 ± 0.5	450 ± 60	81 ± 3
2†	K_m, V_{max}, c	Ade K_i‡	4.6 ± 0.4	500 ± 40	79 ± 1

Data from Fig. 3 were analyzed by nonlinear regression as described in Materials and Methods. Parameters are those obtained for the fit of the appropriate equation to the data ± SEM for the fit.

* Data in the absence of Ade.

† All data.

‡ Ade K_i was 12 μM [25].

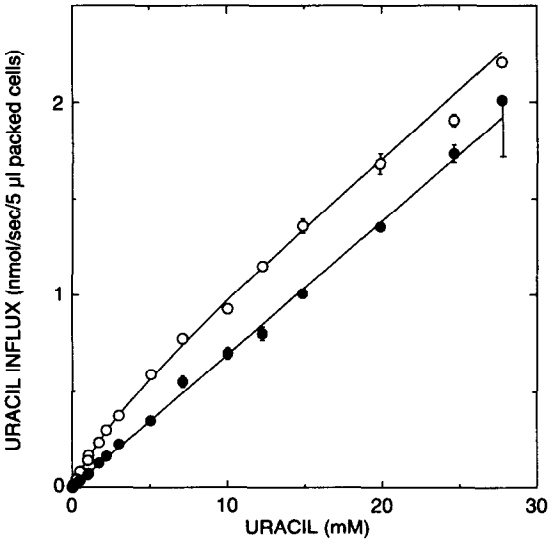

Fig. 4. Concentration dependence of Ura influx. Assays were performed at 37° in the absence (○) or presence (●) of 3.0 mM Ade. [^{3}H]Ura concentrations were 5.0 μM to 28 mM (0.45 or 41 Ci/mol) and data analysis was as described in the legend of Fig. 3.

cases, the P values (>0.08) indicated that the more complex model of noncompetitive inhibition did not fit the data significantly better than the simpler model of competitive inhibition. 5-FU influx was competitively inhibited by Ade or Hyp (Fig. 5, Table 3), and 5-FU competitively inhibited the influx of Ade or Hyp (Fig. 6, Table 3). Ura influx was competitively inhibited by Ade or Hyp, and Ura competitively inhibited Ade or Hyp influx (Table 3). In all cases, K_i values were similar to the respective K_m values for influx.

DISCUSSION

The "inhibitor-stop" assay was effective for determining initial rates of influx of 5-FU and Ura in human erythrocytes at 37°. The influx of both 5-FU and Ura was nonconcentrative and significantly, but not completely, inhibited by nucleobases. Moreover, the partial inhibition of influx by 3.0 mM

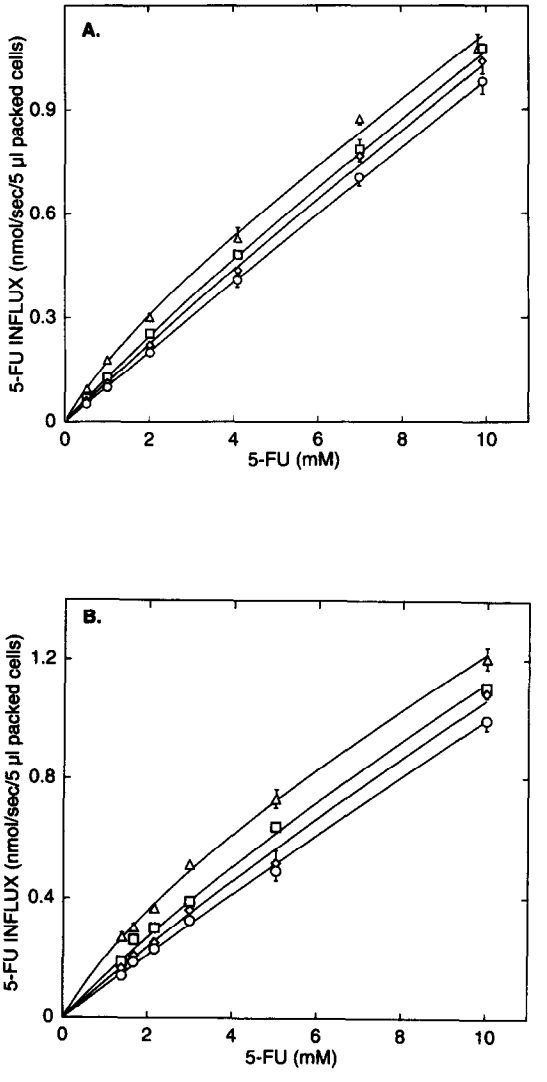

Fig. 5. Inhibition of 5-FU influx by (A) Ade and (B) Hyp. Assays were performed at 37°. Curves were derived by nonlinear regression analysis for competitive inhibition using Equation 2 in Materials and Methods for (A) [^{3}H]5-FU (1.0 Ci/mol) influx in the absence (△) or presence of 10 (□), 20 (◇), or 50 (○) μM Ade, P value = 1.000, and (B) [^{3}H]5-FU (0.51 Ci/mol) influx in the absence (△) or presence of 180 (□), 360 (◇), or 720 (○) μM Hyp, P value = 0.4316. Error bars are as described in the legend of Fig. 3.

Table 3. Kinetic parameters for the influx into human erythrocytes of 5-FU, Ura, Ade, and Hyp

	Permeant influx parameters			Inhibitor K_i (mM)			
Permeant	K_m (mM)	V_{max} (pmol/sec/5 μL cells)	c^* (pmol/sec/mM/5 μL cells)	5-FU	Ura	Ade	Hyp
5-FU	4.0 ± 0.4 (5)	530 ± 80 (5)	81 ± 2* (3)	ND	ND	0.009 ± 0.002 (3)	0.17 ± 0.03 (2)
Ura	5.8 ± 0.7 (4)	480 ± 60 (4)	77 ± 6* (2)	ND	ND	0.010 ± 0.003 (2)	0.08 ± 0.04† (1)
Ade	0.011 ± 0.001 (2)	21 ± 4 (2)	240 ± 20‡	3.4 ± 0.6 (2)	4.5 ± 1§ (1)	ND	ND
Hyp	0.24 ± 0.03 (4)	200 ± 30 (4)	100 ± 1‡	3.9 ± 0.5 (3)	5.3 ± 0.2 (2)	ND	ND

The initial velocity of influx of each radiolabeled permeant was determined at 37° as described under Materials and Methods. Inhibitors were added simultaneously with the permeants. Nonlinear regression analysis was performed as described in Materials and Methods using Equations 1, 2 and 3. Numbers in parentheses are the number of determinations with ND being not determined. Values where $N > 2$ are the mean ± SEM of the mean of separate determinations. Values where $N = 2$ are the mean ± the average deviation from the mean. SEM values within each single experiment ranged from 1 to 40% of the K_m value and from 5 to 30% of the V_{max} value.

* The nonfacilitated diffusion constant (c) was determined by linear regression analysis of the slope for the concentration dependence of influx in the presence of 3.0 mM Ade.

† The value ± SEM for the fit of 24 data points to Equation 2 for competitive inhibition.

‡ Data from Ref. 25.

§ The value ± SEM for the fit of 20 data points to Equation 2 for competitive inhibition.

Fig. 6. Inhibition of (A) Ade or (B) Hyp influx by 5-FU. Assays were performed at 37° as described in Materials and Methods, and data were analyzed as described in the legend of Fig. 5 for (A) [^{3}H]Ade (240 Ci/mol) influx in the absence (△) or presence of 2.0 (□), 4.0 (◇), or 8.0 (○) mM 5-FU, P value = 0.1727, and (B) [^{3}H]Hyp (6.1 Ci/mol) influx in the absence (△) or presence of 3.0 (□), 6.0 (◇), or 12 (○) mM 5-FU, P value = 0.0551. Error bars are as described in the legend of Fig. 3.

Ade could not be further enhanced by the addition of pyrimidines or inhibitors of nucleoside transport. This suggestion of two permeation pathways was further supported by the appearance of a saturable and nonsaturable component of influx for both permeants (Figs. 3 and 4). This biphasic nature of 5-FU and Ura influx was highly reproducible and was observed in 4–5 separate experiments. Kinetic analysis also revealed that 5-FU, Ura, Ade, and Hyp were mutually competitive inhibitors (Table 3), with K_i values for inhibition approximately equal to the respective K_m values for influx. We therefore conclude that 5-FU and Ura enter human erythrocytes both by nonfacilitated diffusion and by the same carrier that transports the purine nucleobases.

5-FU and Ura interact with the nucleobase carrier

with similar K_m and V_{max} values that are much higher than those observed for purine nucleobases [25]: K_m values are >20-fold higher; V_{max} values are >3-fold higher. Thus, the transport efficiencies (V_{max}/K_m) for 5-FU and Ura via this carrier are markedly lower than those found for the purines.

The nonfacilitated diffusion rate constants for 5-FU and Ura were similar to each other and also to that observed for Hyp [25]. However, at physiological concentrations (1–5 μM), nonfacilitated diffusion would account for approximately 40% of the total Ura influx and <10% of the total Hyp influx. At therapeutically achievable 5-FU concentrations (10 nM–1 mM) [3], nonfacilitated diffusion would also be an important component of 5-FU influx (~40%).

5-FU is slightly ionized at physiological pH (pK_a = 8.1) [7, 9] and has an increased tissue half-life at pH values below 6.9 [11]. Since the pH of solid tumors is generally acidic [32], we assessed the characteristics of 5-FU influx at pH 6.5 and found kinetic parameters for the nucleobase carrier and the nonfacilitated diffusion rate constant which were similar to those determined at pH 7.3 (data not shown). These observations are consistent with other reports that 5-FU uptake did not vary significantly in this pH region [7, 9].

Plagemann *et al.* [24] reported a saturable component of Ura transport in human erythrocytes, with a K_m similar to the value found in this study. However, these investigators did not recognize the nonfacilitated diffusion component for Ura influx. Consequently, they could not determine the number of independent transporters operative for Ura, Ade, and Hyp influx and, based on a perceived lack of inhibition by Hyp on Ade or Ura influx, they suggested that Ura, Ade, and Hyp use independent nucleobase carriers. Nevertheless, their inhibition results are consistent with those expected from the kinetic parameters and magnitude of nonfacilitated diffusion determined in the present study. For example, at 500 μM Ura, influx via nonfacilitated diffusion would be 44% of the total, leaving 56% of the total as carrier-mediated influx; Plagemann *et al.* [24] observed 47% inhibition of Ura influx by Hyp, which is consistent with the expected inhibition of carrier-mediated influx if Ura and Hyp share the same carrier with the K_m values reported in Table 3. Our results are consistent with another report on human erythrocytes [33] that also recognized a nonsaturable mechanism for 5-FU influx.

Previous studies with Ura or 5-FU in cultured cells, tissues, tumors, or intestinal preparations [4–23] have reported uptake of these compounds by nonfacilitated diffusion, facilitated diffusion, active and concentrative mechanisms, or combinations of these. Most of these studies were performed at longer times which may have been outside the linear velocity region and where significant metabolism may have occurred. However, the reported trapping of nonmetabolized 5-FU in tumors but not in normal tissues is intriguing [12–14]. Transport mechanisms for 5-FU could be different in tumor cells and this may be therapeutically relevant.

Acknowledgements—We gratefully acknowledge Dr. Thomas Spector, Dr. David Porter, and Gregory Corbin for their valuable assistance in the nonlinear regression analyses.

REFERENCES

1. Bleiberg H, Treatment of advanced colorectal cancer. *Anticancer Res* **9**: 1013–1016, 1989.
2. Parker WB and Cheng YC, Metabolism and mechanism of action of 5-fluorouracil. *Pharmacol Ther* **48**: 381–395, 1990.
3. Weckbecker G, Biochemical pharmacology and analysis of fluoropyrimidines alone and in combination with modulators. *Pharmacol Ther* **50**: 367–424, 1991.
4. Zylka JM and Plagemann PGW, Purine and pyrimidine transport by cultured Novikoff cells. *J Biol Chem* **250**: 5756–5767, 1975.
5. Plagemann PGW, Marz R and Wohlhueter RM, Uridine transport in Novikoff rat hepatoma cells and other cell lines and its relationship to uridine phosphorylation and phosphorolysis. *J Cell Physiol* **97**: 49–72, 1978.
6. Marz R, Wohlhueter RM and Plagemann PGW, Purine and pyrimidine transport and phosphoribosylation and their interaction in overall uptake by cultured mammalian cells. *J Biol Chem* **254**: 2329–2338, 1979.
7. Wohlhueter RM, McIvor RS and Plagemann PGW, Facilitated transport of uracil and 5-fluorouracil, and permeation of orotic acid into cultured mammalian cells. *J Cell Physiol* **104**: 309–319, 1980.
8. Jacquez JA, Permeability of Ehrlich cells to uracil, thymine and fluorouracil. *Proc Soc Exp Biol Med* **109**: 132–135, 1962.
9. Kessel D and Hall TC, Studies on drug transport by normal human leukocytes. *Biochem Pharmacol* **16**: 2395–2403, 1967.
10. Yamamoto S and Kawasaki T, Active transport of 5-fluorouracil and its energy coupling in Ehrlich ascites tumor cells. *J Biochem (Tokyo)* **90**: 635–642, 1981.
11. Guerquin-Kern JL, Leteurtre F, Croisy A and Lhoste JM, pH Dependence of 5-fluorouracil uptake observed by *in vivo* ^{31}P and ^{19}F nuclear magnetic resonance spectroscopy. *Cancer Res* **51**: 5770–5773, 1991.
12. Wolf W, Presant CA, Servis KL, El-Tahtawy A, Albright MJ, Barker PB, Ring R, Atkinson D, Ong R, King M, Singh M, Ray M, Wiseman C, Blayney D and Shani J, Tumor trapping of 5-fluorouracil: *In vivo* ^{19}F NMR spectroscopic pharmacokinetics in tumor-bearing humans and rabbits. *Proc Natl Acad Sci USA* **87**: 492–496, 1990.
13. Presant CA, Wolf W, Albright MJ, Servis KL, Ring R, Atkinson D, Ong RL, Wiseman C, King M, Blayney D, Kennedy P, El-Tahtawy A, Singh M and Shani J, Human tumor fluorouracil trapping: Clinical correlations of *in vivo* ^{19}F nuclear magnetic resonance spectroscopy pharmacokinetics. *J Clin Oncol* **8**: 1868–1873, 1990.
14. El-Tahtawy A and Wolf W, *In vivo* measurements of intratumoral metabolism, modulation, and pharmacokinetics of 5-fluorouracil, using ^{19}F nuclear magnetic resonance spectroscopy. *Cancer Res* **51**: 5806–5812, 1991.
15. Schanker LS and Tocco DJ, Active transport of some pyrimidines across the rat intestinal epithelium. *J Pharmacol Exp Ther* **128**: 115–121, 1960.
16. Muranishi S, Yoshikawa H and Sezaki H, Absorption of 5-fluorouracil from various regions of gastrointestinal tract in rat. Effect of mixed micelles. *J Pharmacobiodyn* **2**: 286–294, 1979.
17. Sasaki H, Nakamura J, Konishi R and Shibasaki J, Intestinal absorption characteristics of 5-fluorouracil,

Ftorafur, and 6-mercaptopurine in rats. *Chem Pharm Bull (Tokyo)* **34**: 4265–4272, 1986.
18. Bronk JR and Hastewell JG, The transport of pyrimidines into tissue rings cut from rat small intestine. *J Physiol (Lond)* **382**: 475–488, 1987.
19. Smith P, Mirabelli C, Fondacaro J, Ryan F and Dent J, Intestinal 5-fluorouracil absorption: Use of Ussing chambers to assess transport and metabolism. *Pharm Res* **5**: 598–603, 1988.
20. Katgely BW, Bridges RJ and Rummel W, Inhibition of the intestinal transport of uracil by hexoses and amino acids. *Biochim Biophys Acta* **862**: 429–434, 1986.
21. Bronk JR, Lister N and Lynch S, Absorption of 5-fluorouracil and related pyrimidines in rat small intestine. *Clin Sci* **72**: 705–716, 1987.
22. Schanker LS and Jeffrey JJ, Active transport of foreign pyrimidines across the intestinal epithelium. *Nature* **190**: 727–728, 1961.
23. Schanker LS and Tocco DJ, Some characteristics of the pyrimidine transport process of the small intestine. *Biochim Biophys Acta* **56**: 469–473, 1962.
24. Plagemann PGW, Woffendin C, Puziss MB and Wohlhueter RM, Purine and pyrimidine transport and permeation in human erythrocytes. *Biochim Biophys Acta* **905**: 17–29, 1987.
25. Domin BA, Mahony WB and Zimmerman TP, Purine nucleobase transport in human erythrocytes. *J Biol Chem* **264**: 9276–9284, 1988.
26. Zimmerman TP, Mahony WB and Prus KL, 3′-Azido-3′-deoxythymidine, an unusual nucleoside analogue that permeates the membrane of human erythrocytes and lymphocytes by nonfacilitated diffusion. *J Biol Chem* **262**: 5748–5754, 1987.
27. Paterson ARP, Kolassa N and Cass CE, Transport of nucleoside drugs in animal cells. *Pharmacol Ther* **12**: 515–536, 1981.
28. Domin BA, Mahony WB and Zimmerman TP, 2′,3′-Dideoxythymidine permeation of the human erythrocyte membrane by nonfacilitated diffusion. *Biochem Biophys Res Commun* **154**: 825–831, 1988.
29. Domin BA, Mahony WB, Koszalka GW, Porter DJT, Hajian G and Zimmerman TP, Membrane permeation characteristics of 5′-modified thymidine analogues. *Mol Pharmacol* **41**: 950–956, 1992.
30. Motulsky HJ and Ransnas LA, Fitting curves to data using nonlinear regression: A practical and nonmathematical review. *FASEB J* **1**: 365–374, 1987.
31. Zimmerman TP, Wolberg G and Duncan GS, Inhibition of lymphocyte-mediated cytolysis by 3-deazaadenosine: Evidence for a methylation reaction essential to cytolysis. *Proc Natl Acad Sci USA* **75**: 6220–6224, 1978.
32. Tannock IF and Rotin D, Acid pH in tumors and its potential for therapeutic exploitation. *Cancer Res* **49**: 4373–4384, 1989.
33. Uchida M, Ho DHW, Kamiya K, Yoshimura T, Sasaki K, Tsutani H and Nakamura T, Transport and intracellular metabolism of fluorinated pyrimidines in cultured cell lines. *Adv Exp Med Biol* **253B**: 321–326, 1989.